Adsorption-Induced Deformation of Zeolites 4A and 13X:

Experimental and Molecular Simulation Study

Alina Emelianova,[†] Christian Balzer,[‡] Gudrun Reichenauer,[‡] and Gennady Y. Gor^{*,†}

†Otto H. York Department of Chemical and Materials Engineering

New Jersey Institute of Technology, University Heights, Newark, NJ 07102, USA

‡Center for Applied Energy Research, Magdalene-Schoch-Str. 3, Wuerzburg 97074,

Germany

E-mail: gor@njit.edu

Abstract

Gas adsorption in zeolites leads to adsorption-induced deformation, which can significantly impact the adsorption and diffusive properties of the system. In this study, we conducted both experimental investigations and molecular simulations to understand the deformation of zeolites 13X and 4A during carbon dioxide adsorption at 273 K. To measure the sample's adsorption isotherm and strain simultaneously, we used a commercial sorption instrument with a custom-made sample holder equipped with a dilatometer. Our experimental data showed that while the zeolites 13X and 4A exhibited similar adsorption isotherms, their strain isotherms differed significantly. To gain more insight into the adsorption process and adsorption-induced deformation of these zeolites, we employed a coupled Monte Carlo and molecular dynamics simulations with atomistically detailed models of the frameworks. Our modeling results were consistent with the experimental data and helped us identify reasons behind the different deformation behavior of the considered structures. Our study also revealed the sensitivity of the strain isotherm of zeolites to pore size and other structural and energetic features, suggesting that measuring adsorption-induced deformation could serve as a complementary method for material characterization and provide guidelines for related technical applications.

Introduction

All nanoporous materials deform during the adsorption process due to the interactions between the adsorbate and the surface of a material, this phenomenon is known in the literature as "adsorption-induced deformation". ^{1,2} The extent of deformation can be affected by a number of factors, such as the size and shape of the pore, the surface chemistry of the material, and the properties of the fluid being adsorbed. Microporous materials, with a pore size less than 2 nm, typically exhibit higher adsorption stress in the pores compared to such stress in mesopores ³ due to more significant intermolecular interactions between adsorbate and a pore wall.

Adsorption-induced deformation in zeolites, natural or synthetic microporous aluminosilicates with a wide variety of chemical compositions and structures, have been studied experimentally in a number of works. ^{1,4–15} These studies have shown that the magnitude of deformation in a zeolite structure depends on the zeolite and adsorbate's nature, as well as temperature and gas pressure. ^{5,9} Adsorption-induced deformation can significantly impact zeolites' adsorption and diffusion properties, including adsorption capacity, selectivity, and adsorption kinetics. ¹⁶ In particular, deformation affects permeation and selectivity of zeolite membranes, thereby significantly changing the transport through the defects. ^{12,15,17–19} Moreover, adsorption-induced deformation may compromise the structural integrity of the material, which is crucial in high-pressure applications where a zeolite matrix undergoes degradation upon cycling. Therefore, understanding how zeolites deform under various conditions is essential for designing more efficient adsorption systems.

Zeolite LTA4A is commonly used to separate polar from non-polar molecules by permeation, as this zeolite is highly hydrophilic due to its low Si/Al ratio. ²⁰ Since the polarity of both the zeolite framework (which depends on the Si/Al ratio) and the adsorbate produces a significant effect on their interaction, these features significantly impact the adsorption process and can be some of the largest contributing factors in the deformation process. Additionally, it has been shown that the presence of the framework charges noticeably affects

the framework's structural deformation and fluctuations of the windows in a zeolite. ^{19,21,22} Thus, there is a need to develop a predictive model capable of flexibility toward the systems of different zeolites-adsorbates, as well as the ability to include various system features that can potentially influence the deformation process under different operating conditions.

In the last two decades, there have been several attempts to model the adsorption-induced deformation of zeolites. Jakubov and Mainwaring proposed a model for calculating adsorption stress in zeolites based on the vacancy solution theory. 23 This model applies solution thermodynamics to describe the properties of the adsorbed fluid and calculate the stress in the pore. Ravikovitch and Neimark developed another thermodynamic model, ²⁴ based on the classical density functional theory (DFT), that predicted the strain induced by the adsorption of noble gases in CaNaX zeolite. This model represented zeolite pores as uniform spheres of adjusted pore size to estimate the strain based on the solvation pressure, which matched experimental data. ⁵ However, zeolites can exhibit anisotropy of the deformed framework ^{25,26} that cannot be captured within macroscopic models that consider only normal components of the stress tensor. ²⁷ In complex geometries, the solvation force has both significant normal and tangential components, and the distribution of the solvation force at the solid surface is nonuniform. 28 Therefore, predicting the deformation of a sample as a whole should be considered using a model that can directly predict framework strain, independently of the assumed stress direction. A molecular simulations procedure capable of modeling atomistically detailed flexible zeolite structures upon adsorption would be a more direct approach to predicting the realistic behavior of these materials under different adsorption conditions.

Grand canonical Monte Carlo (GCMC) simulation is a widely used approach to calculate adsorption in porous materials.²⁹ However, since the volume of the system is fixed in the grand-canonical ensemble, the framework size is not allowed to change during the GCMC simulation. As a result, GCMC is not suitable for modeling the deformation of a structure. To simulate adsorption-induced deformation, not only should the number of gas molecules N change during the simulation, but the framework should also be allowed to change its size

under adsorption and external stress. Molecular dynamics (MD) uses an integration of the equations of motion for the guest-loaded framework as a whole, enabling direct sampling of the flexibility of the material. This coupled GCMC-MD approach has become computationally feasible in recent years and has been employed to model the sorption of various fluids in flexible MOFs, ^{30,31} coal, ^{32,33} silica materials, ³⁴ kerogen, ^{35,36} and polymers. ^{37–40} However, only a few studies investigated the zeolite pore shape and size response to the adsorption process by directly sampling the change of the unit cell size with progressing adsorption. For instance, Balestra et al. ⁴¹ applied MC/MD simulations to the system of zeolite RHO-water, and Santander et al. ⁴² focused on silicalite adsorption of furfural-water and hydroxymethyl furfural (HMF)-water mixtures. Nevertheless, none of these studies investigated such effects in FAU and LTA zeolites with experimental validation. Understanding how adsorption affects the structure and properties of these zeolites is essential for optimizing their performance in numerous industrial applications, such as gas separation, catalysis, and ion exchange.

The objective of this study is to enhance the comprehension of adsorption-induced deformation in high aluminum content zeolites such as faujasite (FAU) and Linde Type A (LTA). In this work, we performed molecular simulations to calculate the adsorption of carbon dioxide CO₂ and the corresponding mechanical response of porous frameworks. The experimental data was obtained using in-situ dilatometry measurements of gas adsorption on binderless monolithic zeolites, which is of particular importance for this work for unambiguously attributing the observed adsorption-induced deformation.

A major advantage of this work with respect to previous studies is, firstly, usage of the direct molecular simulation of the fully-coupled adsorption-deformation process in atomistically-detailed models of zeolites, and, secondly, validation of the theoretical predictions of this effect based on high-quality adsorption and strain isotherms obtained by simultaneous measurements of the two processes. The findings of the study are expected to help gain insight into the fundamental interactions that drive adsorption in zeolites, as well as to explore the potential of measuring this effect for materials characterization and to develop guidelines for

related technical applications.

Methods

Zeolite Samples

Zeolites Köstrolith 4A (or LTA4A, LTA-type) and Köstrolith 13X (or NaX, FAU-type) were provided by Chemiewerk Bad Köstritz, Germany. Both zeolites were produced from zeolite powder, metakaolin, and lye, where metakaolin served as a temporary binder for the zeolite powder, which was eventually also converted into zeolite. 43,44 This procedure resulted in binderless monolithic zeolites which was a particularly important feature to be consistent with the simulations models. Frameworks of these zeolites are composed of silicon, aluminum, and oxygen atoms with different Si/Al ratios. Replacing Si with Al results in a negative framework charge which is compensated by sodium cations located on a zeolite surface. LTA4A-type of zeolites exhibits a cubic structure with " α -cages" approximately 11.4 Å in diameter and six circular entrances with a characteristic diameter of 4.1 Å, 45 and with smaller β -cages of 6.6 Å in diameter, separated from α -cages by 2.2 Å apertures. The larger cages ("supercages") in NaX-type exhibit a roughly spherical pore shape of 11.8 Å in diameter with four circular entrances of approximately 7.4 Å. 46

Experimental Details

Zeolite samples were prepared with a nearly spherical shape with a diameter of roughly 1 cm, with a small section flattened by grinding to prevent the samples from rolling in the sample holder. Carbon dioxide (CO₂) adsorption was measured at 273 K using a commercial volumetric adsorption instrument (ASAP2020, Micromeritics). Samples deformation was measured using the in-house built dilatometer, which was integrated into ASAP2020. ⁴⁷ The combined setup, therefore, allows for state-of-the-art adsorption measurements complemented by in-situ dilatometry. ^{48,49} The adsorption instrument and dilatometer ran parallel

without an electronic connection to each other, i.e., ASAP2020 determined the regular adsorption isotherm, while the dilatometer continuously monitored the length of the sample $\ell = \ell(p/p_0)$. The measurement started from the degassed, evacuated and thermally equilibrated state of the sample, at which point the reference length of the sample as seen by the dilatometric setup was ℓ_0 , measured by a caliper. When the degassing was completed, the sample holder was placed in the water-mixed bath with a small amount of glycol connected to a liquid thermostat, controlling the sample temperature during the measurement. The adsorption instrument was measuring the adsorption isotherm, the amount of adsorbed gas divided by the mass of the sample N_a/m as a function of relative pressure p/p_0 . The relation between $\ell(p/p_0)$ and the data points of the adsorption isotherm was determined after the measurement was completed by a simple automated evaluation routine via timestamps as well as separately recorded pressure transducer signals and valve stats. This relation finally resulted in the linear strain isotherm:

$$\varepsilon(p/p_0) = \frac{\ell(p/p_0) - \ell_0}{\ell_0} = \frac{\Delta \ell}{\ell_0}.$$
 (1)

Computational Details

Models

Structures of the zeolites 13X and 4A were modeled according to the crystallographic positions of NaX and LTA4A, respectively, given in the literature. ^{50,51} The crystal structure of the NaX has a dehydrated composition of Na₈₆Al₈₆Si₁₀₆O₃₈₄ with a cubic unit cell dimension of 25.099 Å (schematically shown in Fig. 1a), ⁵⁰ which was constructed by randomly substituting Al atoms with Si atoms according to the Löwenstein's rule. ⁵² The crystal structure for LTA4A was generated with a composition of Na₉₆Al₉₆Si₉₆O₃₈₄ and cubic unit cell dimension of 24.555 Å (schematically shown in Fig. 1b), reported by Pluth et al. ⁵¹ The position of the non-framework cations (Na⁺) inside of a simulation box was generated randomly, and the cations were allowed to move during the simulation. For comparative calculations for

sodium-containing and all-silica frameworks, the all-silica models of the zeolites 4A and 13X were obtained by replacing all Al atoms with Si and removing the Na cations. CO₂ was modeled as a rigid molecule with three charged sites (Table ??), according to the model by Harris and Yung.⁵³ The details of the force field parameters employed to model interactions between the frameworks, Na⁺, and CO₂ are given in the Supporting Information.

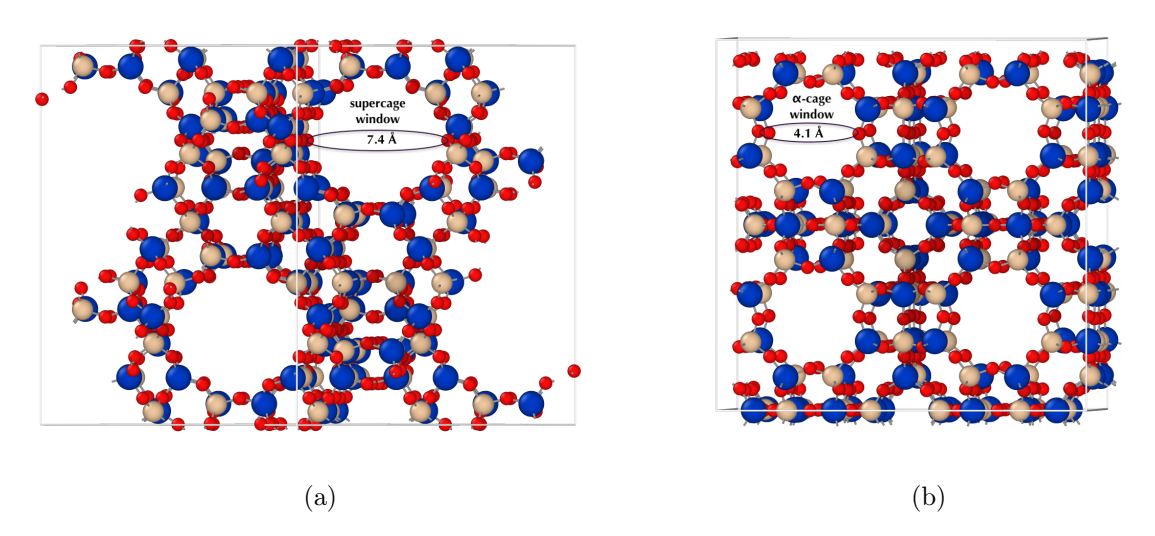


Figure 1: Visualization of the crystallographic structures used to represent the unit cells of zeolites (a) $13X^{50}$ and (b) 4A, ⁵¹ with silicon atoms shown in beige, aluminum in blue and oxygen in red. Visualized with OVITO. ⁵⁴

Molecular Simulations

All simulations were carried out using the open-source software RASPA 2.0. ⁵⁵ Adsorption isotherms were simulated using the Monte Carlo method in the grand canonical ensemble (GCMC), where chemical potential μ , volume V, and temperature T are fixed during the simulation. The GCMC method allows the adsorbate molecules to be moved by translation, rotation, and their exchange between the system and an external gas reservoir at pressure p corresponding to the fixed μ , which were related to each other according to the Peng-Robinson equation of state. ⁵⁶ Accordingly, the vapor pressure p_0 of CO₂ at 273 K was

determined from the Peng-Robinson equation of state (3.46 MPa). The simulations were done for both cases of the rigid and flexible frameworks, allowing the cations to move in both cases. For computational efficiency, in the case of simulations with a rigid structure (GCMC), the internal interactions between framework atoms were excluded, and the adsorbate and Na⁺ only interacted with zeolite oxygen atoms due to its much higher polarizability compared to other atoms. The cutoff radius for the interactions was set to 12 Å and shifted at that distance.

To simulate the adsorption-induced deformation of a zeolite, a coupled GCMC simulation and molecular dynamics (MD) simulation in NPT ensemble scheme was used, with a fully flexible model of a zeolite framework allowing local anisotropic changes of the structure as well as an isotropic change of cell dimensions. The following simulation protocol was employed (Fig. 2):

- 1. A flexible structure was relaxed with the applied force field for 50 ps with the MD simulation in the NPT ensemble to get an equilibrium structure, at T = 273 K and P = 1 bar. Interactions between all zeolite atoms were included, as well as the interactions between the adsorbate and cations with all atoms of the framework. Barostat and thermostat were modeled using the Nosé-Hoover chain method with a time scale parameter of 0.15 ps. ⁵⁷ Cutoff 10 Å was applied (2 Å smaller than half of a box size, to account for a possible shrinking of a unit cell), and the potentials were shifted at the cutoff distance. The final configuration was used to start a coupled MC-MD run.
- 2. The GCMC simulation with a flexible model (all interactions were included) was performed for 2×10^4 cycles. The resulting configuration was used to start the MD simulation in NPT ensemble for 2×10^3 steps, with a time step 1 fs. The same barostat and thermostat settings were used as in Step 1.
- 3. After the MD simulation was finished, the GCMC simulation started from the resulting configuration, and the procedure was repeated until the equilibrium state had been

achieved. The equilibrium was indicated by an equilibrated amount of adsorption and a size of a unit cell, for each pressure p (evolution in time of the average amount of adsorbed molecules and the unit cell size is given in the Supporting Information). It should be noted that the pressure p imposed at the reservoir in GCMC simulation is different from the solvation pressure P acting inside a pore. The difference between these two values defines effective stress in the pore.³⁵

4. The average adsorbed amount N and the average length of the unit cell d were computed based on averaging over the second half of the MC-MD iterations, and the error was estimated as the standard deviation of the values. The reference value d_0 was taken based on the average length corresponding to the lowest pressure considered.

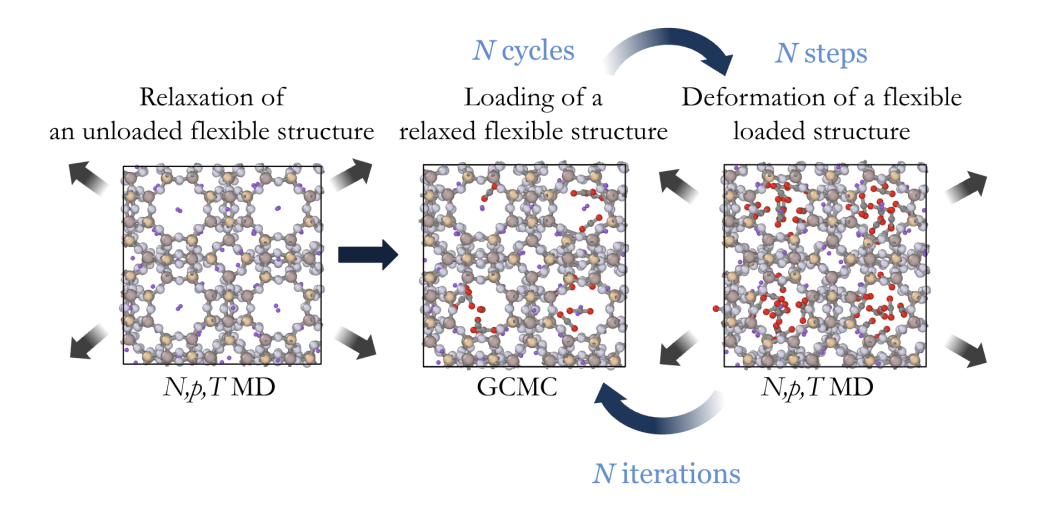


Figure 2: The algorithm of the coupled MC-MD simulation employed to simulate the adsorption-induced deformation of zeolite frameworks. The snapshot on the left represents the flexible zeolite framework being relaxed in the NPT ensemble with no adsorbate present. The purple spheres represent Na⁺, depicting its equilibrium positions in the center of the windows. The middle and right snapshots show a coupled MC-MD iteration with a flexible framework loaded with CO_2 molecules (red and grey spheres). The unit cell volume is constrained in GCMC and unconstrained in MD. Visualized with OVITO.⁵⁴

Since it was essential to assess the accurate description of the mechanical properties of zeolites, we verified the bulk modulus of the dry zeolite structures. The values were estimated as the classical force field zero Kelvin elastic constants by optimizing a unit cell's atomic positions and size based on the generalized Hessian matrix obtained from Baker eigenvector-following method.⁵⁸ The elastic constants were then obtained from the derived Hessian matrix.⁵⁹

Accessible volume was estimated as $V = \phi_{\text{void}} \times V_{\text{cell}}$, where porosity ϕ_{void} of a dry sample was calculated from Monte Carlo simulations of a helium probe. The helium probe can be simulated with the Widom particle insertion method, ⁶⁰ where an attempt to insert a particle into the system is performed and the energy change is evaluated. The void fraction is then calculated based on the obtained average Rosenbluth weight of helium. ⁶¹ The pore volume of a sample as a function of pressure was calculated using the same method by removing the adsorbate molecules from a structure resulting from the coupled MC-MD calculations.

Results and Discussion

Models Validation

The amount of adsorbed CO₂ as a function of gas pressure in the zeolites 4A and 13X at 273 K measured experimentally is shown in Fig. 3. The isotherms for both zeolites are very similar in the relative pressure range $p/p_0 < 10^{-4}$ showing approximately logarithmic dependence between the amount adsorbed and pressure. Overall, at the highest gas pressure of $p/p_0 = 3 \times 10^{-2}$ 13X exhibited higher adsorption of 158 cm³(STP)/g compared to the loading of 4A of 110 cm³(STP)/g, which was consistent with the previous studies. ⁶²

To validate the suitability of the employed models for the simulations of coupled CO_2 adsorption and frameworks deformation, we first simulated the adsorption of CO_2 using the GCMC ensemble and rigid zeolites frameworks and compared them with experimentally measured adsorption isotherms. Fig. 3 shows the calculated isotherms along with experimental data. The simulation predicted a slightly lower amount of adsorption (140 cm³(STP)/g) than obtained experimentally for CO_2 -13X system at $p/p_0 = 3 \times 10^{-2}$. For 4A, the simulation

also underestimated total adsorption showing a maximum loading of 91 cm³(STP)/g. The disagreement in the maximum amount of adsorbed gas between simulation and experiment may be, firstly, due to not rigorous parameterization of combined force field parameters: the partial charges of the frameworks were taken from Nicholas et al. force field parameterized to reproduce structural properties (theoretical infrared spectra) of silicalite, ⁶³ and the other parameters were developed independently to reproduce CO₂ adsorption on zeolites. ⁶⁴ Additionally, the deviation of the simulations for both systems at low relative pressures is likely due to the chemisorption of CO₂ in the experiment, which has been reported to occur in high Al and Na⁺ containing zeolites ^{65,66} and was not taken into account within the non-reactive force field. This effect, however, should not affect simulated strains of the frameworks qualitatively, as the non-reactive models are still able to describe the orientation of the adsorbate molecules and the energy contribution of different adsorption sites. However, the quantitative accuracy of these predictions may be limited due to the lack of chemical bonding interactions.

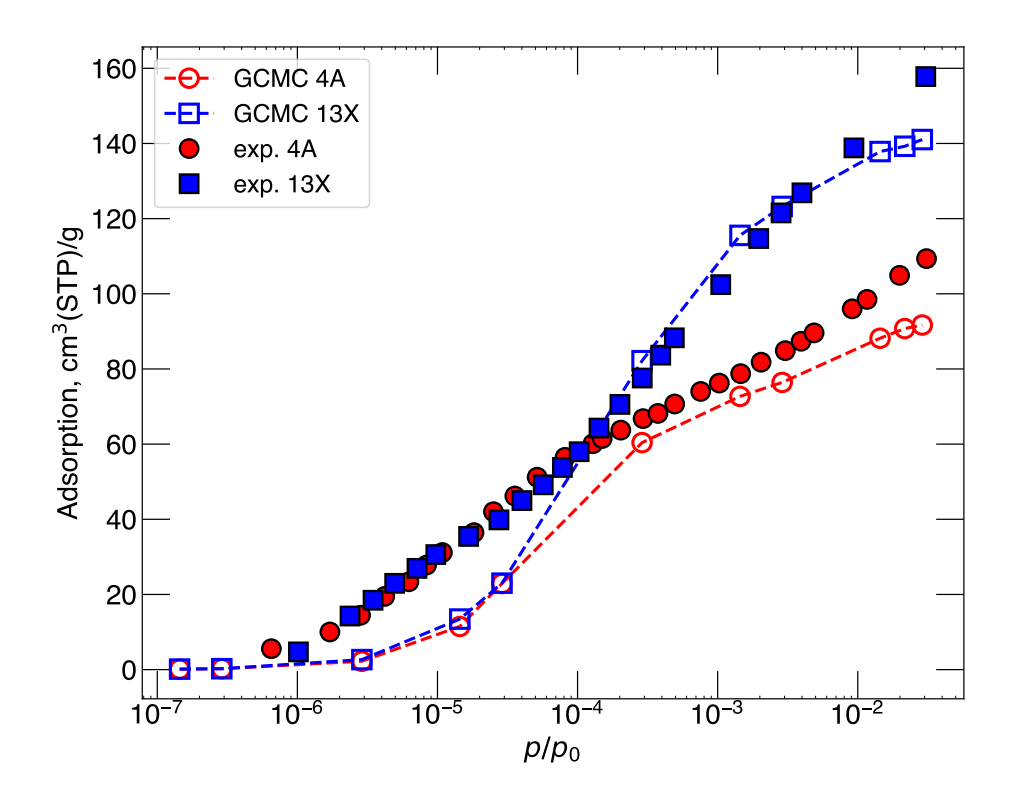


Figure 3: Experimental adsorption isotherms on zeolites samples (filled markers) and the isotherms simulated with the GCMC method (dashed line with empty markers) for CO₂ at 273 K (logarithmic scale).

The bulk moduli of the zeolites were calculated to benchmark the accuracy of simulating the mechanical properties of the structures. Results are shown in Table 1 in comparison with the experimentally measured bulk modulus of 13 X.⁶⁷ The calculations predicted the bulk modulus of 13X with only a slight deviation of 5%. For 4A, the bulk modulus value was only available for a different unit cell formula (Ref. 68). Based on the result obtained for 13X, it was concluded that the employed models give an adequate description of the mechanics of the considered zeolites.

Table 1: Bulk modulus of zeolites obtained with Baker minimization (this work) in comparison with experimental data

	K, GPa	
	this work	exp.
4A	38.0	-
13X	36.0	38.0^{67}

Adsorption-Induced Deformation

Figure 4 presents the experimental and simulated strain of samples as a function of relative CO_2 pressure. The experimental data show, despite a very similar adsorption isotherm (Fig. 3), a distinctively different fingerprint in adsorption deformation below about $p/p_0 =$ 4×10^{-4} , that is qualitatively confirmed by the simulations. The zeolite 13X sample contracted at low pressure $(p/p_0 = 2 \times 10^{-5})$ with a negative strain of $\varepsilon = 9 \times 10^{-4}$ and gradually expanded at higher pressures $(p/p_0 = 3 \times 10^{-4})$. In the simulation, the strain was measured relative to the state at $p/p_0=3\times 10^{-7}$ (where no adsorption was observed experimentally) with a reference unit cell length d_0 . The simulated strain of 13X exhibited significant contraction till $p/p_0 = 10^{-3}$, with the minimum strain of approximately -28×10^{-4} at $p/p_0 = 2 \times 10^{-5}$. This deformation pattern is consistent with the previous in-situ dilatometry studies on faujasite zeolites 5,69 and theoretical studies of deformation of microporous materials. ^{24,70} The contraction occurring at low pressures may be explained as the long-ranged attraction between CO_2 molecules and the zeolite wall. 71,72 At this stage of adsorption, the attractive forces between the molecules and the walls dominate the free energy of the system, 70 causing an adsorbate molecule to act as a bridge between opposite adsorption sites and the structure to contract. The mechanism differs from the contraction observed in mesoporous materials, where at low adsorption amounts, the localization of adsorbed molecules can lead to the contracting surface stresses. 73,74

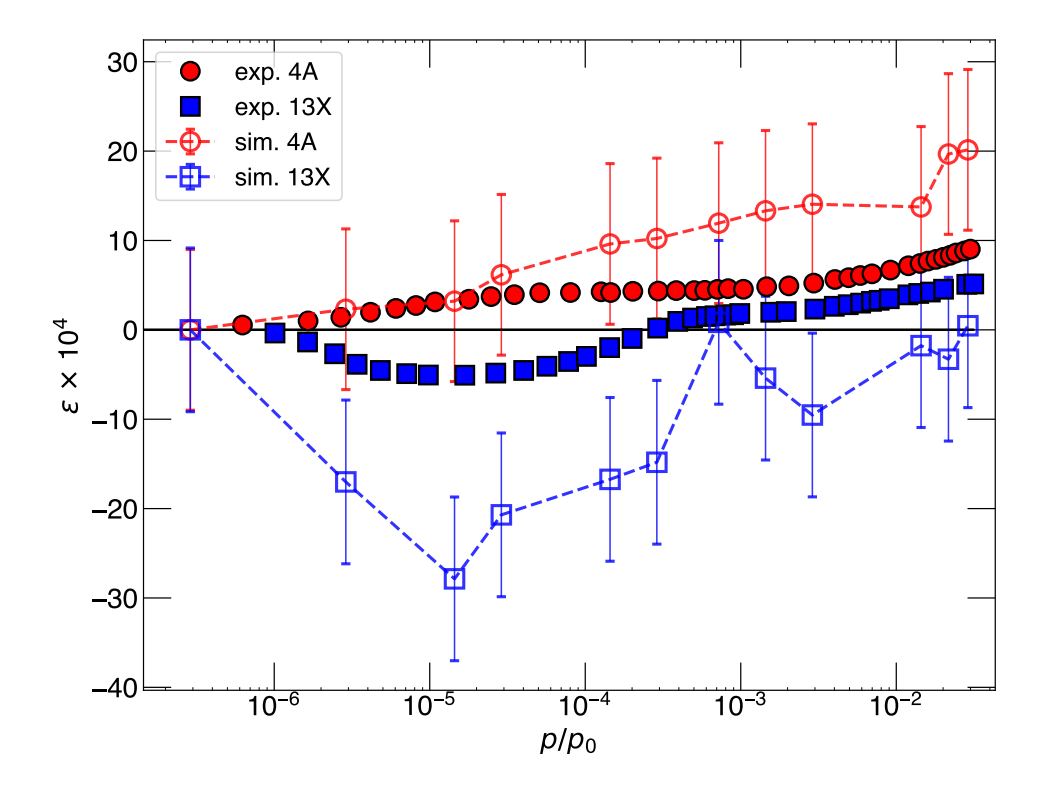


Figure 4: Experimental (filled markers) and simulated (dashed line with empty markers) strain isotherms for zeolites 4A and 13X upon adsorption of CO₂ at 273 K (logarithmic scale). For the experimental data, the error bars are less than the marker size. The black solid line shows zero strain level for clarity.

To explain the appearance of the minimum of 13X strain isotherm, the positions of Na⁺, CO₂, and framework atoms were analyzed with varying pressure in the coupled MC-MD simulations. From the radial distribution functions (RDFs) calculated based on the MC part of the simulations shown in Figure 5, it was found that the distance between Na⁺ in 13X does not change throughout adsorption (Fig. 5a), while the distance between Na⁺ and the Al atoms in 13X initially decreases, reaching the minimum distance of 3.39 Å (Fig. 5c). The decreasing distance causes electrostatic repulsion between the positively charged Al and Na⁺. Hence, due to the restricted movement of Na⁺ when the pore is filled with CO₂, the increasing electrostatic repulsion between the framework and Na⁺ causes the framework to expand in order to accommodate the adsorbed molecules.

Unlike for zeolite 13X, experimentally measured strain of 4A showed a monotonic expan-

sion over the entire pressure range, reaching a maximum of $\varepsilon = 9 \times 10^{-4}$ at the maximum loading (Figure 4). The simulations showed a similar trend, although the magnitude of the predicted strain was twice higher. This deformation trend of 4A not only differs from 13X but also qualitatively differs from the previous studies of adsorption-induced deformation of zeolites: a theoretical investigation based on classical DFT by Ravikovitch and Neimark ²⁴ for the pore of a similar size (1.5 nm) showed that zeolites contract in the regime of low pressure which agreed with previous experimental findings for zeolite CaNaX; ⁵ additionally, Eskandari-Ghadi and Zhang using surface poromechanics model showed that the contraction in the low-pressure regime is in general expected for materials with sufficiently small pores at sufficiently low gas pressures, ⁷⁰ due to surface tension competing over disjoining pressure in the free energy of the system. These theories have also been supported by several previous experimental studies on zeolites deformation. ^{69,75,76} Therefore, this behavior of 4A required additional clarification, which can be obtained by comparing the results with the behavior of the all-silica zeolites.

The simulated strain isotherms for all-silica zeolites, where all Al atoms of the framework were replaced by Si is shown in Fig. ??. All-silica 4A showed contraction until the pressure of $p/p_0 = 2 \times 10^{-3}$, followed by expansion according to a mechanism similar to the one exhibited by 13X at high pressures. Hence, the presence of Na⁺ cations and their location in the 4A framework was linked to the expansion appearing even at the early stage of adsorption. The structure of 4A is known to have a "trap-door" mechanism for CO₂ molecules due to the Na⁺ occupying the 8-membered window of an α -cage with a diameter of 0.41 nm. This limits the diffusion of CO₂ through the pores of 4A and further restricts its mobility and packing, ⁷⁷ including the necessity to temporarily displace the cation from the window of an α -cage, ⁷⁸ which additionally promotes the expansion of the framework. In contrast, zeolite 13X has a larger window size with cations located at the center of the hexagonal prisms, with two sites inside the sodalites (β -cages), and other three sites inside the supercages, ⁷⁹ and thus a larger Na⁺-Na⁺ distance. In 13X, only the migration of the cations to the nearby sites was

observed according to the mechanism described by Plant et al.⁸⁰ Moreover, the all-silica NaX (Fig. ??), exhibited contraction which continues even at higher pressures of $p/p_0 = 2 \times 10^{-3}$, contrary to 13X. This suggests that the expansion of 13X at high pressures happens due to the repulsion between the framework and cations, similar to the mechanism in 4A.

To confirm that the presence of Na⁺ and their positions inside framework cause 4A expansion, we analyzed the radial distribution functions of 4A framework atoms, Na⁺, and CO₂ (Fig. 5). The Na⁺ ions were on average significantly closer to each other in 4A, with an average distance of 4.9 $\mathring{\rm A}$ which is shorter than any known or predicted dual-cation sites 77,81 (Fig. 5a-5b), compared to the average distance of 5.9 Å in 13X. The reason for this difference is that the size of the windows in the α -cages of 4A zeolite is smaller compared to the size of the windows in the supercages of the 13X zeolite, as well as due to the preferable location of the cations, resulting in more tightly packed Na⁺ and fewer space available for their movement upon progressing CO_2 loading. Additionally, it was found that the sodium ions moved closer to the framework atoms, creating more space for the CO₂ molecules, which contributed to further expansion of the framework: the obtained RDFs (Fig. 5c-5d) for Na⁺-Al pair showed that the most populated distance between them decreased from 3.59~Å to 3.51 Å with increasing pressure. The distance between a pair of cations in 4A increased slightly with increasing pressure (Fig. 5b), and the distance between Na⁺ ions and CO₂ molecules (Fig. 5e-5f) remained relatively constant of about 2.9 Å which corresponds to the optimal distance of the two-site complexes in 4A. 82,83

We should also comment on the noticeable deviation of the simulation results from the experimental curves, overestimating the maximum expansion of the 4A framework by a factor of two and the maximum contraction of 13X by a factor of four. Fig. ?? shows the adsorption isotherms extracted from the coupled MC-MD simulations, the results are shown in comparison with the previously shown result based on the GCMC simulation (where the rigid frameworks models were used). Additionally, Fig. ?? shows the strain isotherms with the calculations in the low-pressure range $p/p_0 < 3 \times 10^{-7}$. The coupled

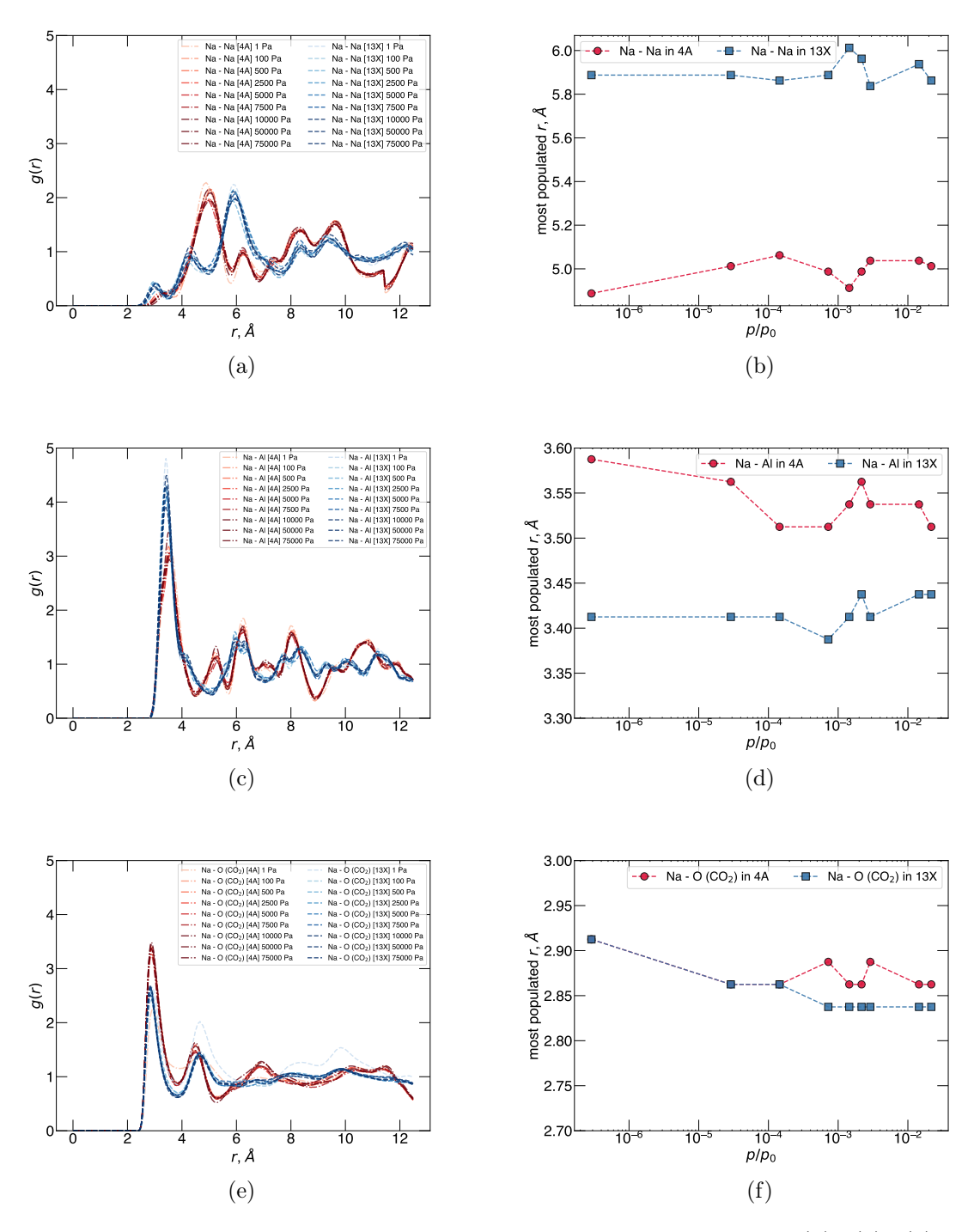


Figure 5: RDFs calculated based on the coupled MC-MD simulations (a), (c), (e) and the corresponding plots of the relative atoms distances where the RDFs peaks are located (b), (d), (f) at each relative pressure point (logarithmic scale), for Na–Na, Na–Al, and Na–O (CO₂) pairs, respectively.

MC-MD approach showed adsorption below the relative pressure of 10^{-6} for both zeolites, compared to GCMC simulations and experiments where no adsorption was observed at such low pressures. This caused the simulated strain isotherms shown in Figure 4 to be shifted toward lower pressure compared to the experimental curves. This discrepancy can be attributed to a problematic combination of two different force fields that describe framework flexibility (bonded parameters and partial charges for zeolites parameterized to reproduce structural properties) and adsorption (van der Waals parameters fitted to reproduce CO_2 adsorption) coupled with the presence of extra framework cations. We verified that replacing the partial charges with those offered in the force field by Ref. 84 changes the results only slightly within the error bars.

Notably, isotherms extracted from MC-MD simulations showed such simulation inaccuracy for only 13X and 4A, while all-silica models exhibited isotherms with zero adsorption at low relative pressures according to experimental measurements. ⁸⁵ Ref. 84 mentioned that adsorption of CO₂ in high Al/Si zeolites significantly perturbs the Si-O-Al angle. The distribution and corresponding variance of the bonds and angles in our simulations of 4A (Figure ??) and 13X (Figure ??) showed that even at low pressure, the variance from the equilibrium bond lengths was significant and increased with pressure, and the variance for Si-O-Al was higher for both zeolites. The O-Al bond was perturbed more significantly at low pressure, which may have caused the deviation from the adsorption in the rigid structures due to the lack of original parameterization by Nicholas et al. ⁶³ In addition, the difference in total loading obtained in the MC-MD simulations is attributed to the fact that the unit cell volume obtained after applying the force field and allowing the structure to relax was lower than the initial structure based on crystallographic data.

Moreover, the reason for the inaccuracy of the simulated isotherms at low pressures, where chemisorption is more likely to occur, was that the force field used in the simulation does not consider the formation of chemical bonds between the gas molecules and the zeolite framework. It has been described in the literature previously that simulations of

the cationic zeolites often exhibit deviations from the experiment due to the inability to accurately describe cation mobility and include chemisorption effects (within a non-reactive force field). 84,86 These issues indicate that there is a more rigorous parameterization required to quantitatively reproduce the mechanics of a zeolite framework with cations while simulating an adsorption process. The main goal of the simulations conducted in the current study, however, was to reveal a principal difference in the mechanical response of zeolites to adsorption, and to qualitatively describe it at the molecular level. Based on the obtained simulations results, it can be concluded that the trend in the adsorption-induced strain of the zeolites of types LTA and FAU mostly depends on the architecture of a framework and the location of the extra-framework cations, causing different energy contributions driving the deformation process, which was observed both at the macro and micro levels.

It is important to note that the deformation perturbs the volumes of the solid and of the pore space independently, 87 and a single scalar strain value may not appropriately describe the deformation of a sample as a whole and only capture the overall trend. This can be a primary reason for the quantitative difference between measured and simulated strain isotherms. Here, it was mainly important to verify that there is no inconsistency between the change of the unit cell size and a change in the pores volume, hence, the accessible pore volume of the simulated structures was plotted as a function of relative pressure (Fig. 6). To clarify, the volume V corresponds to the resulting configuration obtained from the coupled MC-MD simulation, and V_0 is this value obtained for the lowest pressure point. The change of the volume $V-V_0$ is shown in comparison with the strain observed in the last MC-MD cycle (which slightly deviated from the average strain shown previously in Fig. 4). Contraction of the 13X unit cell led to the reduction of the volume of the pores and expansion of the 4A framework led to its increasing, relative to the initial V_0 state. At several points (e.g. $p/p_0 = 3 \times 10^{-6}$ for 4A and $p/p_0 = 3 \times 10^{-3}$ for 13X), where the unit cell was increasing in size, the pore volume decreased, which can be attributed to the deformation of the regions inaccessible to CO_2 but accessible for the helium probe. In general, the unit cell strain appeared consistent with the change of the pore volume with pressure for both zeolites.

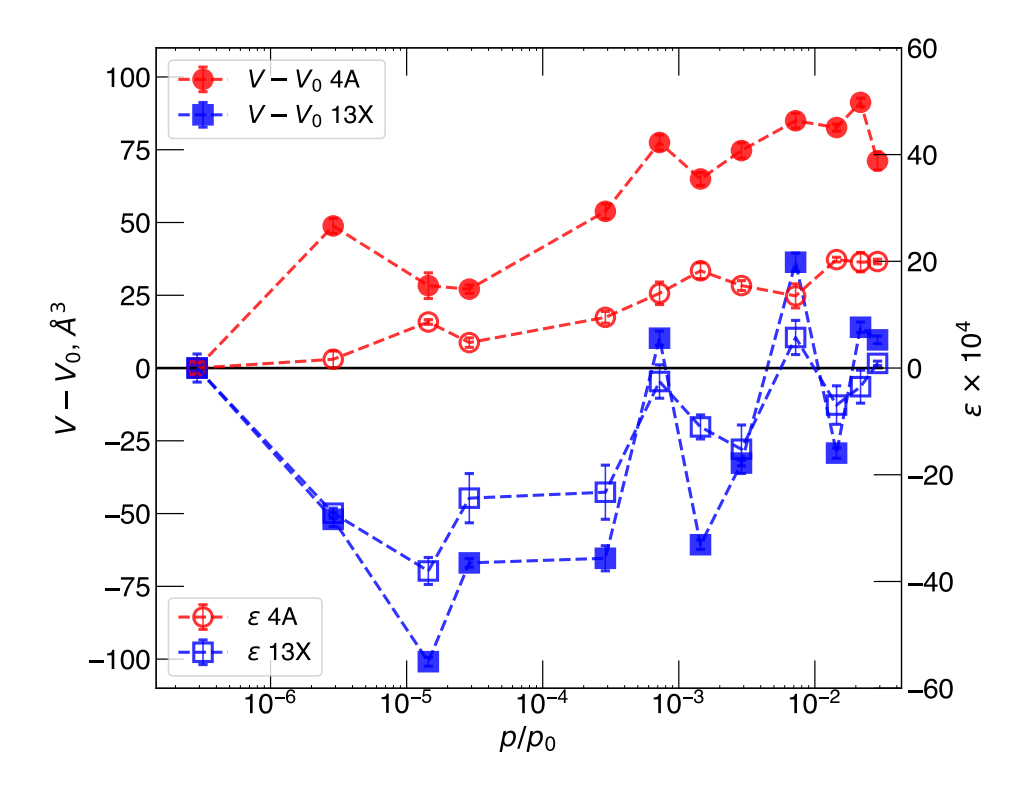


Figure 6: Change of the pore volume of zeolites framework as a function of gas pressure (in logarithmic scale) relative to the pore volume of a dry structure V_0 at 273 K (full symbols) and the strain of a zeolite unit cell (open symbols). The black solid line shows zero strain level for clarity.

The fundamentally different responses to the adsorption in the porous structure of the two zeolites which are similar in the size of the super cages, chemical composition, and pore wall density indicated the complexity of this phenomenon and dependence on details of a zeolite porous structure. Therefore, a thermodynamic theory for the prediction of the adsorption-induced deformation in zeolites may not be able to take into account features that could potentially impact the deformation and give a realistic prediction of this process. The results of this work demonstrated the ability of the molecular simulations to reproduce the main trends in the adsorption-induced strain of the samples with different driving forces of deformation. Specific features of a structure, such as a framework topology and the location of the charge-balancing cations, were shown to affect the deformation mechanism, thus it

will be particularly important to include these features in the model of the systems with polar adsorbates such as water which capable of causing a substantial dislodge of cations. ⁸⁸ Thus, for a specific system zeolite-adsorbate of interest, an atomistically-detailed simulation based on known crystallographic data of a structure with well-parameterized models would be required, to give an accurate prediction of its adsorption-induced deformation at specific operating conditions.

Conclusion

In conclusion, we measured the deformation of zeolites 4A and 13X upon adsorption of carbon dioxide and found that they have qualitatively different dependence on gas pressure. Zeolite 13X exhibited contraction at low pressures and expansion at high pressures of the adsorbing gas, a behavior typical for many microscopic materials. However, the 4A zeolite, while exhibiting a similar adsorption isotherm, showed a monotonic expansion when adsorption progresses. The results were supported by coupled Monte Carlo and molecular dynamics simulations, demonstrating similar trends of the deformation of the unit cell of the structures. The difference in the deformation patterns of the two structures was attributed to the limitations of the pores size and interactions of the extra-framework sodium cations with the adsorbate molecules. At the early stage of adsorption, when the pore is loosely filled with the adsorbate, the adsorbing molecules can exert negative stress on the pore walls and, thus, contraction of materials, as was observed for 13X. In another scenario, as was shown for 4A, there can be a monotonic expansion of a zeolite framework observed in the entire range of imposed gas pressures. We showed that this effect is caused by (1) the windows size of 4A being comparable in size with CO₂ molecule, creating less space for adsorbate mobility, and (2) the presence of extra-framework cations, causing the adsorbed molecule to produce short-ranged repulsion rather than long-range attraction at the early stage of adsorption. The key findings in this work offer valuable insights into the behavior of FAU

and LTA types of zeolites under adsorption and provide a basis for further studies in the field of adsorption-induced deformation of microporous materials.

Acknowledgement

The authors thank Dr. Yafan Yang (King Abdullah University of Science and Technology) for providing an example of the simulation algorithm and Dr. Peter Ravikovitch (ExxonMobil) for useful discussions. This work was supported by the National Science Foundation (CBET-1944495 to G.Y.G.)

Supporting Information

- Input files (RASPA format) and scripts used for coupled GCMC/MD simulations (ZIP)
- Force field description and additional simulations results (PDF)

References

- (1) Gor, G. Y.; Huber, P.; Bernstein, N. Adsorption-induced deformation of nanoporous materials A review. *Appl. Phys. Rev.* **2017**, *4*, 011303.
- (2) Vandamme, M. Coupling between adsorption and mechanics (and vice versa). Curr. Opin. Chem. Eng. 2019, 24, 12–18.
- (3) Kowalczyk, P.; Furmaniak, S.; Gauden, P. A.; Terzyk, A. P. Carbon dioxide adsorption-induced deformation of microporous carbons. *J. Phys. Chem. C* **2010**, *114*, 5126–5133.
- (4) Bering, B.; Krasil'nikova, O.; Sarakhov, A.; Serpinskii, V.; Dubinin, M. Alteration of zeolite granule dimensions under krypton adsorption. Bull. Acad. Sci. USSR, Div. Chem. Sci. 1977, 26, 2258–2261.

- (5) Krasil'nikova, O.; Bering, B.; Serpinskii, V.; Dubinin, M. Deformation of zeolite CaNaX during xenon adsorption. *Russ. Chem. Bull.* **1977**, *26*, 1099–1101.
- (6) Mentzen, B.; Gelin, P. The silicalite/p-xylene system: part I—flexibility of the MFI framework and sorption mechanism observed during p-xylene pore-filling by X-ray powder diffraction at room temperature. *Mater. Res. Bull.* 1995, 30, 373–380.
- (7) Van Koningsveld, H.; Jansen, J. Single crystal structure analysis of zeolite H-ZSM-5 loaded with naphthalene. *Microporous Mater.* **1996**, *6*, 159–167.
- (8) Nair, S.; Tsapatsis, M. The location of o-and m-xylene in silicalite by powder X-ray diffraction. J. Phys. Chem. B **2000**, 104, 8982–8988.
- (9) Pulin, A.; Fomkin, A.; Sinitsyn, V.; Pribylov, A. Adsorption and adsorption-induced deformation of NaX zeolite under high pressures of carbon dioxide. Russ. Chem. Bull. 2001, 50, 60–62.
- (10) Lee, Y.; Vogt, T.; Hriljac, J. A.; Parise, J. B.; Artioli, G. Pressure-induced volume expansion of zeolites in the natrolite family. *J. Am. Chem. Soc.* **2002**, *124*, 5466–5475.
- (11) Fomkin, A.; Shkolin, A.; Pulin, A.; Men'shchikov, I.; Khozina, E. Adsorption-induced deformation of adsorbents. *Colloid J.* **2018**, *80*, 578–586.
- (12) Sorenson, S. G.; Smyth, J. R.; Kocirik, M.; Zikanova, A.; Noble, R. D.; Falconer, J. L. Adsorbate-induced expansion of silicalite-1 crystals. *Ind. Eng. Chem. Res.* 2008, 47, 9611–9616.
- (13) Lee, J. B.; Funke, H. H.; Noble, R. D.; Falconer, J. L. High selectivities in defective MFI membranes. J. Membr. Sci. 2008, 321, 309–315.
- (14) Lee, J. B.; Funke, H. H.; Noble, R. D.; Falconer, J. L. Adsorption-induced expansion of defects in MFI membranes. *J. Membr. Sci.* **2009**, *341*, 238–245.

- (15) Sorenson, S. G.; Payzant, E. A.; Gibbons, W. T.; Soydas, B.; Kita, H.; Noble, R. D.; Falconer, J. L. Influence of zeolite crystal expansion/contraction on NaA zeolite membrane separations. *J. Membr. Sci.* **2011**, *366*, 413–420.
- (16) Pérez-Botella, E.; Valencia, S.; Rey, F. Zeolites in Adsorption Processes: State of the Art and Future Prospects. *Chem. Rev.* **2022**, *122*, 17647–17695.
- (17) Sorenson, S. G.; Smyth, J. R.; Noble, R. D.; Falconer, J. L. Correlation of crystal lattice expansion and membrane properties for MFI zeolites. *Ind. Eng. Chem. Res.* 2009, 48, 10021–10024.
- (18) Sorenson, S. G.; Payzant, E. A.; Noble, R. D.; Falconer, J. L. Influence of crystal expansion/contraction on zeolite membrane permeation. *J. Membr. Sci.* **2010**, *357*, 98–104.
- (19) Ilić, B.; Wettstein, S. G. A review of adsorbate and temperature-induced zeolite framework flexibility. *Microporous Mesoporous Mater.* **2017**, *239*, 221–234.
- (20) Castillo, J. M.; Silvestre-Albero, J.; Rodriguez-Reinoso, F.; Vlugt, T. J.; Calero, S. Water adsorption in hydrophilic zeolites: experiment and simulation. *Phys. Chem. Chem. Phys.* 2013, 15, 17374–17382.
- (21) Smirnov, K. S.; Bougeard, D. A molecular dynamics computer study of window fluctuations in zeolite A. *Zeolites* **1994**, *14*, 203–207.
- (22) Bueno-Pérez, R.; Calero, S.; Dubbeldam, D.; Ania, C. O.; Parra, J. B.; Zaderenko, A. P.; Merkling, P. J. Zeolite force fields and experimental siliceous frameworks in a comparative infrared study. J. Phys. Chem. C 2012, 116, 25797–25805.
- (23) Jakubov, T. S.; Mainwaring, D. E. Adsorption-induced dimensional changes of solids. *Phys. Chem. Chem. Phys.* **2002**, *4*, 5678–5682.

- (24) Ravikovitch, P. I.; Neimark, A. V. Density functional theory model of adsorption on amorphous and microporous silica materials. *Langmuir* **2006**, *22*, 11171–11179.
- (25) Coudert, F.-X. Systematic investigation of the mechanical properties of pure silica zeolites: stiffness, anisotropy, and negative linear compressibility. *Phys. Chem. Chem. Phys.* **2013**, *15*, 16012–16018.
- (26) Gaillac, R.; Chibani, S.; Coudert, F.-X. Speeding up discovery of auxetic zeolite frameworks by machine learning. *Chem. Mater.* **2020**, *32*, 2653–2663.
- (27) Emelianova, A.; Maximov, M. A.; Gor, G. Y. Solvation pressure in spherical mesopores: Macroscopic theory and molecular simulations. *AIChE J.* **2021**, *67*, e16542.
- (28) Shi, K.; Smith, E. R.; Santiso, E. E.; Gubbins, K. E. A perspective on the microscopic pressure (stress) tensor: History, current understanding, and future challenges.

 J. Chem. Phys. 2023, 158, 040901.
- (29) Gubbins, K. E.; Liu, Y.-C.; Moore, J. D.; Palmer, J. C. The role of molecular modeling in confined systems: impact and prospects. *Phys. Chem. Chem. Phys.* **2011**, *13*, 58–85.
- (30) Jawahery, S.; Simon, C. M.; Braun, E.; Witman, M.; Tiana, D.; Vlaisavljevich, B.; Smit, B. Adsorbate-induced lattice deformation in IRMOF-74 series. *Nat. Commun.* 2017, 8, 13945.
- (31) Zhang, L.; Hu, Z.; Jiang, J. Sorption-induced structural transition of zeolitic imidazolate framework-8: A hybrid molecular simulation study. *J. Am. Chem. Soc.* **2013**, *135*, 3722–3728.
- (32) Zhang, J.; Clennell, M.; Dewhurst, D.; Liu, K. Combined Monte Carlo and molecular dynamics simulation of methane adsorption on dry and moist coal. *Fuel* **2014**, *122*, 186–197.

- (33) Zhang, J.; Liu, K.; Clennell, M.; Dewhurst, D.; Pervukhina, M. Molecular simulation of $CO_2 CH_4$ competitive adsorption and induced coal swelling. Fuel **2015**, 160, 309–317.
- (34) Chen, M.; Coasne, B.; Guyer, R.; Derome, D.; Carmeliet, J. Molecular simulation of sorption-induced deformation in atomistic nanoporous materials. *Langmuir* **2019**, *35*, 7751–7758.
- (35) Ho, T. A.; Wang, Y.; Criscenti, L. J. Chemo-mechanical coupling in kerogen gas adsorption/desorption. *Phys. Chem. Chem. Phys.* **2018**, *20*, 12390–12395.
- (36) Wu, J.; Huang, P.; Maggi, F.; Shen, L. Molecular investigation on CO₂ CH₄ displacement and kerogen deformation in enhanced shale gas recovery. Fuel 2022, 315, 123208.
- (37) Dutta, R. C.; Bhatia, S. K. Transport diffusion of light gases in polyethylene using atomistic simulations. *Langmuir* **2017**, *33*, 936–946.
- (38) Palmer, J. C.; Debenedetti, P. G. Computer simulation of water sorption on flexible protein crystals. J. Phys. Chem. Lett. 2012, 3, 2713–2718.
- (39) Morgan, W. J.; Anstine, D. M.; Colina, C. M. Temperature Effects in Flexible Adsorption Processes for Amorphous Microporous Polymers. J. Phys. Chem. B 2022, 126, 6354–6365.
- (40) Yang, Y.; Narayanan Nair, A. K.; Sun, S. Sorption and diffusion of methane and carbon dioxide in amorphous poly (alkyl acrylates): a molecular simulation study. J. Phys. Chem. B 2020, 124, 1301–1310.
- (41) Balestra, S. R.; Gutiérrez-Sevillano, J. J.; Merkling, P. J.; Dubbeldam, D.; Calero, S. Simulation study of structural changes in zeolite RHO. J. Phys. Chem. C 2013, 117, 11592–11599.

- (42) Santander, J. E.; Tsapatsis, M.; Auerbach, S. M. Simulating adsorptive expansion of zeolites: Application to biomass-derived solutions in contact with silicalite. *Langmuir* **2013**, *29*, 4866–4876.
- (43) Brandt, A.; Schmeisser, J.; Unger, B.; Tschritter, H.; Henkel, U.; Bálint, G.; Gruhle, D.; Winterstein, G. Adsorptionsmittelgranulat und Verfahren zu dessen Herstellung. Patentus EP2249 961B1, 2010.
- (44) Schumann, K.; Brandt, A.; Unger, B.; Scheffler, F. Bindemittelfreie zeolithische Molekularsiebe der Typen LTA und FAU. *Chem. Ing. Tech.* **2011**, *83*, 2237–2243.
- (45) Hazen, R. Zeolite molecular sieve 4A: anomalous compressibility and volume discontinuities at high pressure. *Science* **1983**, *219*, 1065–1067.
- (46) Baerlocher, C.; McCusker, L. Database of Zeolite Structures. 2010; http://www.iza-structure.org/databases/, accessed: 2023/03/01.
- (47) Reichenauer, G.; Scherer, G. Extracting the pore size distribution of compliant materials from nitrogen adsorption. *Colloids Surf. A: Physicochem. Eng. Asp.* **2001**, *187*, 41–50.
- (48) Balzer, C.; Wildhage, T.; Braxmeier, S.; Reichenauer, G.; Olivier, J. P. Deformation of porous carbons upon adsorption. *Langmuir* **2011**, *27*, 2553–2560.
- (49) Balzer, C. Adsorption-Induced Deformation of Nanoporous Materials in-situ Dilatometry and Modeling. PhD dissertation, Julius-Maximilians-Universität Würzburg, 2017.
- (50) Olson, D. H. The crystal structure of dehydrated NaX. Zeolites 1995, 15, 439–443.
- (51) Pluth, J. J.; Smith, J. V. Accurate redetermination of crystal structure of dehydrated zeolite A. Absence of near zero coordination of sodium. Refinement of silicon, aluminumordered superstructure. J. Am. Chem. Soc. 1980, 102, 4704–4708.
- (52) Loewenstein, W. The distribution of aluminum in the tetrahedra of silicates and aluminates. Am. Min. 1954, 39, 92–96.

- (53) Harris, J. G.; Yung, K. H. Carbon dioxide's liquid-vapor coexistence curve and critical properties as predicted by a simple molecular model. *J. Phys. Chem.* **1995**, *99*, 12021–12024.
- (54) Stukowski, A. Visualization and analysis of atomistic simulation data with OVITO-the Open Visualization Tool. *Model. Simul. Mater. Sci. Eng.* **2009**, *18*, 015012.
- (55) Dubbeldam, D.; Calero, S.; Ellis, D. E.; Snurr, R. Q. RASPA: molecular simulation software for adsorption and diffusion in flexible nanoporous materials. *Mol. Simul.* **2016**, *42*, 81–101.
- (56) Peng, D.-Y.; Robinson, D. B. A new two-constant equation of state. *Ind. Eng. Chem. Fundam.* **1976**, *15*, 59–64.
- (57) Martyna, G. J.; Klein, M. L.; Tuckerman, M. Nosé–Hoover chains: The canonical ensemble via continuous dynamics. *J. Chem. Phys.* **1992**, *97*, 2635–2643.
- (58) Baker, J. An algorithm for the location of transition states. J. Comput. Chem. 1986, 7, 385–395.
- (59) Burtch, N. C.; Heinen, J.; Bennett, T. D.; Dubbeldam, D.; Allendorf, M. D. Mechanical properties in metal-organic frameworks: emerging opportunities and challenges for device functionality and technological applications. Adv. Mater. 2018, 30, 1704124.
- (60) Widom, B. Some topics in the theory of fluids. J. Chem. Phys. 1963, 39, 2808–2812.
- (61) Talu, O.; Myers, A. L. Molecular simulation of adsorption: Gibbs dividing surface and comparison with experiment. *AIChE J.* **2001**, *47*, 1160–1168.
- (62) Siriwardane, R. V.; Shen, M.-S.; Fisher, E. P.; Poston, J. A. Adsorption of CO₂ on molecular sieves and activated carbon. *Energy & Fuels* **2001**, *15*, 279–284.

- (63) Nicholas, J. B.; Hopfinger, A. J.; Trouw, F. R.; Iton, L. E. Molecular modeling of zeolite structure. 2. Structure and dynamics of silica sodalite and silicate force field. *J. Am. Chem. Soc.* **1991**, *113*, 4792–4800.
- (64) García-Sánchez, A.; Dubbeldam, D.; Calero, S. Modeling adsorption and self-diffusion of methane in LTA zeolites: the influence of framework flexibility. J. Phys. Chem. C 2010, 114, 15068–15074.
- (65) Bonenfant, D.; Kharoune, M.; Niquette, P.; Mimeault, M.; Hausler, R. Advances in principal factors influencing carbon dioxide adsorption on zeolites. Sci. Technol. Adv. Mater. 2008, 9, 013007.
- (66) Liu, Q.; Mace, A.; Bacsik, Z.; Sun, J.; Laaksonen, A.; Hedin, N. NaKA sorbents with high CO₂-over-N₂ selectivity and high capacity to adsorb CO₂. Chem. Commun. 2010, 46, 4502–4504.
- (67) Colligan, M.; Forster, P. M.; Cheetham, A. K.; Lee, Y.; Vogt, T.; Hriljac, J. A. Synchrotron X-ray powder diffraction and computational investigation of purely siliceous zeolite Y under pressure. J. Am. Chem. Soc. 2004, 126, 12015–12022.
- (68) Arletti, R.; Ferro, O.; Quartieri, S.; Sani, A.; Tabacchi, G.; Vezzalini, G. Structural deformation mechanisms of zeolites under pressure. *Am. Mineral.* **2003**, *88*, 1416–1422.
- (69) Fomkin, A. Adsorption of gases, vapors and liquids by microporous adsorbents. *Adsorption* **2005**, *11*, 425–436.
- (70) Eskandari-Ghadi, M.; Zhang, Y. Mechanics of shrinkage-swelling transition of microporous materials at the initial stage of adsorption. *Int. J. Solids Struct.* 2021, 222, 111041.
- (71) Balzer, C.; Cimino, R. T.; Gor, G. Y.; Neimark, A. V.; Reichenauer, G. Deformation

- of microporous carbons during N_2 , Ar, and CO_2 adsorption: Insight from the density functional theory. Langmuir **2016**, 32, 8265–8274.
- (72) Neimark, A. V.; Grenev, I. Adsorption-induced deformation of microporous solids: a new insight from a century-old theory. *J. Phys. Chem. C* **2019**, *124*, 749–755.
- (73) Gor, G. Y.; Bernstein, N. Adsorption-induced surface stresses of the water/quartz interface: Ab initio molecular dynamics study. *Langmuir* **2016**, *32*, 5259–5266.
- (74) Gor, G. Y.; Bernstein, N. Revisiting Bangham's law of adsorption-induced deformation: changes of surface energy and surface stress. *Phys. Chem. Chem. Phys.* 2016, 18, 9788–9798.
- (75) Lakhanpal, M.; Flood, E. Stresses and strains in adsorbate—adsorbent systems: IV. Contractions of activated carbon on adsorption of gases and vapors at low initial pressures. Can. J. Chem. 1957, 35, 887–899.
- (76) Balzer, C.; Morak, R.; Erko, M.; Triantafillidis, C.; Hüsing, N.; Reichenauer, G.; Paris, O. Relationship between pore structure and sorption-induced deformation in hierarchical silica-based monoliths. *Z Phys. Chem.* (N F) **2015**, 229, 1189–1209.
- (77) Bae, T.-H.; Hudson, M. R.; Mason, J. A.; Queen, W. L.; Dutton, J. J.; Sumida, K.; Micklash, K. J.; Kaye, S. S.; Brown, C. M.; Long, J. R. Evaluation of cation-exchanged zeolite adsorbents for post-combustion carbon dioxide capture. *Energy Environ. Sci.* 2013, 6, 128–138.
- (78) Cheung, O.; Wardecki, D.; Bacsik, Z.; Vasiliev, P.; McCusker, L. B.; Hedin, N. Highly selective uptake of carbon dioxide on the zeolite |Na_{10.2} KCs_{0.8}|-LTA-a possible sorbent for biogas upgrading. *Phys. Chem. Chem. Phys.* **2016**, *18*, 16080–16083.
- (79) Martin-Calvo, A.; Parra, J.; Ania, C.; Calero, S. Insights on the anomalous adsorption of carbon dioxide in LTA zeolites. *J. Phys. Chem. C* **2014**, *118*, 25460–25467.

- (80) Plant, D.; Maurin, G.; Jobic, H.; Llewellyn, P. Molecular dynamics simulation of the cation motion upon adsorption of CO₂ in faujasite zeolite systems. *J. Phys. Chem. B* **2006**, *110*, 14372–14378.
- (81) Findley, J. M.; Ravikovitch, P. I.; Sholl, D. S. The effect of aluminum short-range ordering on carbon dioxide adsorption in zeolites. *J. Phys. Chem. C* **2018**, *122*, 12332–12340.
- (82) Zukal, A.; Arean, C.; Delgado, M.; Nachtigall, P.; Pulido, A.; Mayerová, J.; Cejka, J. Combined volumetric, infrared spectroscopic and theoretical investigation of CO₂ adsorption on Na-A zeolite. *Microporous Mesoporous Mater.* 2011, 146, 97–105.
- (83) Rzepka, P.; Wardecki, D.; Smeets, S.; Muüller, M.; Gies, H.; Zou, X.; Hedin, N. CO₂-induced displacement of Na⁺ and K⁺ in zeolite |NaK|-A. J. Phys. Chem. C **2018**, 122, 17211–17220.
- (84) Garcia-Sanchez, A.; Ania, C. O.; Parra, J. B.; Dubbeldam, D.; Vlugt, T. J.; Krishna, R.; Calero, S. Transferable force field for carbon dioxide adsorption in zeolites. J. Phys. Chem. C 2009, 113, 8814–8820.
- (85) Palomino, M.; Corma, A.; Rey, F.; Valencia, S. New Insights on CO₂- Methane separation using LTA zeolites with different Si/Al ratios and a first comparison with MOFs. Langmuir 2010, 26, 1910–1917.
- (86) Fang, H.; Demir, H.; Kamakoti, P.; Sholl, D. S. Recent developments in first-principles force fields for molecules in nanoporous materials. *J. Mater. Chem.A* **2014**, *2*, 274–291.
- (87) Gor, G. Y.; Huber, P.; Weissmüller, J. Elastocapillarity in nanopores: Sorption strain from the actions of surface tension and surface stress. *Phys. Rev. Materials* **2018**, *2*, 086002.

(88) Joos, L.; Swisher, J. A.; Smit, B. Molecular simulation study of the competitive adsorption of H₂O and CO₂ in zeolite 13X. *Langmuir* **2013**, 29, 15936–15942.

TOC Graphic

